

The temperature dependence of interlayer exchange coupling - spin waves vs. spacer effects

S. Schwieger, J. Kienert, and W. Nolting

Lehrstuhl Festkörperteorie, Institut für Physik, Humboldt-Universität zu Berlin, Newtonstr. 15, 12489 Berlin

There are different mechanisms proposed to be responsible for the temperature dependence of the interlayer exchange coupling (IEC), namely a smearing out of the spacer or interface Fermi surface and excitations and interactions of spin waves. We propose a possibility to separate both effects by calculating the excitation spectrum of an extended Heisenberg model and connecting the results with ferromagnetic resonance (FMR) experiments. To solve the Heisenberg model we use an approximation that was shown to yield excellent results. In this paper the main idea of this procedure is explained and a detailed investigation of the spin wave contribution to the temperature dependence of FMR resonance frequencies and fields is carried out.

I. INTRODUCTION

The discovery of the interlayer exchange coupling (IEC) has triggered a renewed interest in the physics of ultrathin metallic films in the last decades. The term IEC denotes the coupling of magnetic layers separated by non magnetic spacer layers that occurs in quite a number of metallic and semiconducting systems.^{1,2} The general mechanism of the coupling and a lot of additional features are well understood today. The coupling is caused by spin dependent reflection of spacer electrons at the magnet/non-magnet interfaces leading to a spin dependent interference and therewith to a spin dependent renormalization of the density of states (DOS) and the free energy within the spacer.¹ The modification of the spacer DOS and energy depends sensitively on the relative orientation of the magnetic layers favoring a special configuration. This results in the interlayer coupling. The coupling may be ferro- or antiferromagnetic and oscillates with respect to the spacer thickness. The periods of the oscillation depend on the spacer Fermi surface, while the amplitudes as well as the phases may be additionally influenced by interface roughness, interdiffusion, disorder, and related effects. However, up to now it is not clear which kind of process dominates the temperature dependence of the coupling. There are several candidates which are evaluated and compared in Ref. 3:

- (i) One source of temperature dependence is connected with the described coupling mechanism and is caused by the smearing out of the Fermi-surface of the spacer.^{4,5} Furthermore temperature influences the reflection coefficients at the magnet/non-magnet interfaces.⁶ Both processes influence the energy of the spacer layer and will be called “spacer effect” in the following.
- (ii) Another source of temperature dependence are magnetic excitations, altering the properties of the magnetic layers⁷ (“magnetic layer effect”). Thermal magnetic disorder may drastically reduce the energy difference between parallel and antiparallel alignment of the magnetic layers and therewith the

interlayer coupling.

To find the dominating mechanism elaborate ferromagnetic resonance (FMR) measurements were performed at a prototype trilayer,^{8,9} namely a Ni₇/Cu_x/Co₂/Cu(001) system where the subscripts denote the number of atomic layers of each film. The data are analyzed using a classical continuum model, where the classical equation of motion for the magnetization¹⁰ or an expansion of the free energy¹¹ is considered. This analysis gives the temperature dependence of an effective interlayer coupling $\tilde{J}_I(T)$ which is discussed in detail in Ref. 12 and reconsidered in Ref. 3. This quantity is proportional to the energy difference between the state where the magnetization of both magnetic films are parallel to each other and the state where the magnetization of the lower magnetic film are aligned antiparallel to the magnetization of the upper one:

$$\tilde{J}_I(T) \sim F_{\uparrow\uparrow}(T) - F_{\uparrow\downarrow}(T). \quad (1)$$

Note that the magnetic moments are supposed to be parallel within the magnetic films. The most important feature of $\tilde{J}_I(T)$ found experimentally is its effective $T^{3/2}$ -like decrease with temperature. Naturally both temperature dependencies, i.e. the temperature dependence due to the Fermi surface softening and those due to magnetic excitations, are included in $\tilde{J}_I(T)$. Thus, since both mechanisms (i) and (ii) contribute, the dominating mechanism cannot be deduced directly from $\tilde{J}_I(T)$.^{3,12}

On the other hand a procedure sensitive to only one of the mechanisms (i) or (ii) would be highly desirable. It would allow to separate the mechanisms and to deduce the source of temperature dependence of the IEC directly from the measurements. It is the intention of this paper to show that such a procedure exists. The new approach is based on an alternative analysis of FMR measurements using the microscopic Heisenberg model.

To illustrate the idea let us consider a modeling of the considered trilayer systems:

$$H = - \sum_{\langle ij \rangle \alpha} J_{\alpha} \mathbf{S}_{i\alpha} \mathbf{S}_{j\alpha} - \sum_{\langle i\alpha j\beta \rangle}^{\alpha \neq \beta} J_I \mathbf{S}_{i\alpha} \mathbf{S}_{j\beta}$$

$$\begin{aligned}
& - \sum_{i\alpha} g_{J\alpha} \mu_B \mathbf{B}_0 \mathbf{S}_{i\alpha} - \sum_{i\alpha} K_{2\alpha} S_{i\alpha}^2 \quad (2) \\
& + \sum_{ij\alpha} g_{0\alpha\beta} \left(\frac{1}{r_{ij}^3} \mathbf{S}_{i\alpha} \mathbf{S}_{j\beta} - \frac{3}{r_{ij}^5} (\mathbf{S}_{i\alpha} \mathbf{r}_{ij})(\mathbf{S}_{j\beta} \mathbf{r}_{ij}) \right),
\end{aligned}$$

where α runs over the two different layers while i and j denote a lattice site within a layer. For convenience the sums in the first lines are taken over nearest neighbors only. Thus the *intralayer* coupling parameters J_α as well as the *interlayer* coupling parameter J_I are effective parameters containing also the contributions of non-nearest-neighbor interactions. The model describes two magnetic layers coupled by the interlayer coupling J_I , which may be positive or negative. The intralayer coupling constants J_α are chosen to be positive to describe ferromagnetic layers. The model further accounts for anisotropies due to spin orbit ($K_{2\alpha}$) and dipolar ($g_{0\alpha}$) coupling as well as for an external field $g_{J\alpha} \mu_B \mathbf{B}_0$ applied in arbitrary direction. The parameter $g_{J\alpha}$ denotes the Landé factor of the layer α . The anisotropy due to spin-orbit coupling $K_{2\alpha}$, which includes magnetocrystalline as well as magnetoelastic contributions,¹³ will often be termed "lattice anisotropy" in the following. The film plane is the xy -plane and tetragonal symmetry is assumed. Such a model is often used to describe magnetic properties of transition metal films,¹⁴ especially in the presence of anisotropies. Note that the spacer of the trilayer system is not considered explicitly but its effects on the magnetic layers are described by the model parameter J_I . The latter is proportional to the energy difference between the states of parallel and antiparallel aligned magnetizations in both layers, $\mathbf{M}_a \uparrow \uparrow \mathbf{M}_b$ and $\mathbf{M}_a \uparrow \downarrow \mathbf{M}_b$, if saturated magnetism is assumed. This applies for $T = 0$ or at finite temperatures for cases where the spin wave excitations of the model (2) are artificially frozen. For the latter case a temperature dependence of J_I can be caused exclusively by excitations within the spacer. Hence, $J_I(T)$ is proportional to the difference between the energy contributions of the *spacer* in the parallel and antiparallel state:

$$J_I(T) \sim F_{\uparrow\uparrow}^{sp}(T) - F_{\uparrow\downarrow}^{sp}(T). \quad (3)$$

Now we want to connect the model (2) with the mentioned FMR experiments. The probed quantity of an FMR experiment is the so called "resonance frequency" that is identical to the spin wave mode with infinite wavelength ω_0 .⁹ This mode is also called uniform ($q = 0$) mode. In a coupled bilayer system there are two such excitations, termed optical and acoustical mode (ω_{0o}, ω_{0a}). This can easily be understood if a semiclassical spin model is considered. The uniform mode of a monolayer corresponds to a spin wave where all spins rotate in phase. The acoustical mode of the coupled bilayer system corresponds to the state where the spins in both layers rotate in phase. If the optical mode is excited, the spins in the upper layer rotate in anti-phase compared to

the spins of the lower layer. Depending on the coupling sign, the optical mode can be found at higher (ferromagnetic interlayer coupling) or at lower frequencies (antiferromagnetic coupling). Note that the FMR technique has equal access to ferromagnetic and antiferromagnetic coupling. In this picture the distance between the modes $\Delta\omega_0$ is a measure for the interlayer coupling strength if equivalent magnetic layers are assumed.

In practice, during an FMR experiment the probe frequency ν_{hf} is fixed in the microwave region, while the magnitude of the external field is varied until the resonance frequency equals the probe frequency.

$$2\pi\nu_{hf} \stackrel{!}{=} \omega_{0(a,o)}(\mathbf{B}_0) \quad (4)$$

This relation is fulfilled at special magnitudes of the external field called "resonance fields" ($B_{0r(a,o)}$). The values of the resonance fields as functions of the direction of the applied external fields ($B_{0r(a,o)}(\theta_{B_0})$) is the most important experimental output.¹⁵ For an appropriately chosen probe frequency there are also two resonance fields in a coupled bilayer system (2) belonging to the optical and acoustical mode. Again, the distance between the resonance fields (ΔB_{0r}) is influenced by the interlayer coupling strength J_I and the anisotropies in both layers. An FMR experiment can be analyzed using the model (2) by calculating the spin wave modes $\omega_{0(a,b)}$ and the resonance fields $B_{0r(a,o)}$ and fitting the model parameters until the calculated values correspond to the measured ones. It is possible to obtain the interlayer coupling as well as the anisotropy strengths from the angular dependence of the resonance fields.

Let us now consider the temperature dependence of the resonance frequencies and fields. There are two principal sources of temperature dependence:

1. If the parameters of the model (2) are fitted to real systems as proposed above, they may be temperature dependent itself. This applies especially to the interlayer coupling parameter J_I which is not a fundamental microscopic coupling constant but rather given in Eq. (3) and which may be significantly influenced by temperature.^{1,16} As seen in Eq. (3) the temperature dependence of $J_I(T)$ describes the temperature dependence of the spacer energies.
2. Additionally, even if the model parameters are fixed, there is an intrinsic temperature dependence of $\omega_{0(a,o)}$ and $\Delta B_{0(a,o)}$ in the model (2) due to interactions of spin waves excited within the magnetic layers.

It is obvious that the temperature dependence of the model parameter $J_I(T)$ can be identified to the "spacer effect" (i) while the intrinsic temperature dependence due to spin wave interactions is equivalent to the "magnetic layer effect" (ii).

In this situation the microscopic model (2) can be used to study the mechanisms (i) and (ii) separately. On the

one hand one can fit the model parameters to experimental FMR data which gives the function $J_I(T)$. The latter exclusively describes the temperature dependence of the IEC due to the “spacer effect” (i).

On the other hand the model parameters and especially J_I can be fixed. Then one can investigate the temperature dependence of the resonance frequencies due to spin wave interactions. Thus the temperature dependence of the FMR signal caused by the magnetic layer effect (ii) alone can be analyzed.

The motivation of our paper is twofold. First we want to show that an evaluation of FMR data is in principle possible by use of the microscopic model (2). However, our paper is mainly dedicated to the investigation of the second point, i.e. of the temperature dependence of the FMR signal caused by the interaction of spin waves.

The paper is organized in the following way:

Using our microscopic model we will discuss two quantities: the resonance frequencies $\omega_{0(a,o)}$ and the resonance fields $B_{0r(a,o)}$. We will consider a monolayer (simulating a single film) as well as a system of two coupled layers (which simulates prototype IEC-trilayer systems). We compare the results of the classical model with those of the microscopic model at zero temperature before we discuss the intrinsic temperature dependence of the resonance frequencies and fields in detail. With this procedure we want to answer the following central questions:

- Is there a relevant intrinsic temperature dependence of the uniform spin wave modes in the model (2) and how is it characterized?
- What are the differences between the results of our microscopic approach and of the macroscopic classical model for zero temperature, in other words, can the microscopic model give new insight in FMR experiments at a fixed temperature, too?

It turns out that the latter is indeed the case. For a nickel films grown on a Cu(001) surface the absence of a resonance field in the hard direction was reported.¹⁷ This observation follows directly for larger out-of-plane lattice anisotropies in the microscopic model, while it can be hardly explained within the classical model. Furthermore we will find a significant temperature dependence of the uniform modes due to spin wave interactions. A description of this temperature dependence in terms of effective model parameters ($\tilde{K}_2(T)$ and $\tilde{J}_I(T)$) is possible approximately only and justified only for lower temperatures $T < T_c$. Before turning to the presentation of our results we will shortly discuss the approximations used to solve the model (2). The intended use poses clear requirements to the theory. Its numerical effort must be moderate to keep the fitting procedure feasible, while it has to yield accurate results for the spin waves for arbitrary directions and magnitudes of the external field. Such a theory is proposed and evaluated in Ref. 18 and applied to our model (2) in the next section. As already mentioned this contribution uses results and insights from earlier works,

namely from Ref. 3 and Ref. 18. The former (Ref. 3) discusses and compares the different mechanisms that may cause a temperature dependence of the interlayer exchange coupling on a very general level therewith clearly formulating the problem we want to consider in this paper. The latter (Ref. 18) is mere technically proposing a theory to solve our model (2).

II. THEORY

In this section we want to motivate the theoretical approach used to solve the extended Heisenberg model (2). Due to the tetragonal symmetry the directions in the film plane are equivalent. This allows us to restrict our calculations to a plane perpendicular to the film, the xz -plane. The external field and the magnetization are confined to this plane in the following:

$$\begin{aligned} \mathbf{B}_0 &= (B_{0x}, 0, B_{0z}) \\ \langle \mathbf{S} \rangle &= (\langle S_x \rangle, 0, \langle S_z \rangle). \end{aligned}$$

To proceed we split the Hamiltonian (2) into two parts. The first one,

$$\begin{aligned} H_1 &= \sum_{\langle ij \rangle \alpha} J_\alpha \mathbf{S}_{i\alpha} \mathbf{S}_{j\alpha} - \sum_{\langle i\alpha j\beta \rangle} J_I \mathbf{S}_{i\alpha} \mathbf{S}_{j\beta} \\ &\quad - \sum_{i\alpha} g_J \mu_B \mathbf{B}_0 \mathbf{S}_{i\alpha} - \sum_{i\alpha} K_{2\alpha} S_{i\alpha z}^2, \end{aligned} \quad (5)$$

contains all terms except for the dipolar coupling. In a previous paper¹⁸ we developed a theory for the Hamiltonian (5) for the special case of a monolayer. It was shown by comparison with Quantum Monte Carlo (QMC) results¹⁹ that our approximation is in fact very accurate for arbitrary directions of the external field and can therefore be used here. Our proposal combines an RPA decoupling procedure²⁰ applied to the nonlocal Heisenberg exchange terms and a generalized Anderson Callen approximation^{21,22} for the local anisotropy term. Details are given in Ref. 18. The theory is based on a transformation into a local coordinate system $\Sigma \rightarrow \Sigma'$ where the new z' -axis is parallel to the magnetization. It is easy to generalize this theory to a multilayer system if the RPA decoupling is also used for the interlayer coupling term. A remarkable result of this theory is that the anisotropy and the interlayer coupling can be replaced by internal fields $\mathbf{B}_{1\alpha}$ in the single magnon Green function matrix of the transformed system:

$$G'_{\alpha\beta\mathbf{q}}(E) = \langle \langle S_{\alpha\mathbf{q}}^{+}; S_{\beta-\mathbf{q}}^{-} \rangle \rangle. \quad (6)$$

The effective field is a sum of the external field, a term due to the anisotropy and a further term resulting from the interlayer coupling:

$$\mathbf{B}_{1\alpha} = g_{J\alpha} \mu_B \mathbf{B}_0 + \mathbf{B}_{K_{2\alpha}} + \mathbf{B}_{J_I \alpha}. \quad (7)$$

The interlayer field is given by

$$\mathbf{B}_{J_1\alpha} = 2J_I p' \langle \mathbf{S}_\gamma \rangle, \quad (8)$$

where p' denotes the number of nearest neighbors in the adjacent layer γ . For the anisotropy field one finds

$$\begin{aligned} B_{K_2\alpha x} &= -K_{2\alpha} \langle S_{\alpha x} \rangle \sin^2 \theta_\alpha C'_1 \\ B_{K_2\alpha z} &= +2K_{2\alpha} \langle S_{\alpha z} \rangle \left(1 - \frac{1}{2} \sin^2 \theta_\alpha \right) C'_1 \\ \text{with} \\ C'_1 &= 1 - \frac{1}{2S^2} (S(S+1) - \langle S_{\alpha z'}^2 \rangle), \end{aligned} \quad (9)$$

where θ_α is the angle between the z -axis and the magnetization in layer α . Note that the anisotropy field \mathbf{B}_{K_2} is not an analytic function of the magnetization $\langle S_{z'} \rangle$ only, but of $\langle S_{z'}^2 \rangle$ -terms as well. The single-magnon Green function (6) is now a functional of the effective fields:

$$\mathbf{G}'_{\mathbf{q}}(E) = \begin{pmatrix} \langle 2S_{\alpha z'} \rangle & 0 \\ 0 & \langle 2S_{\beta z'} \rangle \end{pmatrix} \cdot (E\mathbf{I} - \mathbf{M}_{\mathbf{q}})^{-1},$$

via the matrix $\mathbf{M}_{\mathbf{q}}$:

$$\begin{aligned} M_{\mathbf{q}}^{\alpha\alpha} &= (2J_\alpha \langle S_{\alpha z'} \rangle (p - \gamma_{\mathbf{q}\parallel}) - B_{1\alpha}) \\ M_{\mathbf{q}}^{\alpha\beta} &= (2J_I \langle S_{\beta z'} \rangle \gamma_{\mathbf{q}\perp} \cos(\theta_a - \theta_b)) \\ M_{\mathbf{q}}^{\beta\alpha} &= (M_{\mathbf{q}}^{\alpha\beta})^*. \end{aligned} \quad (10)$$

Generally, the magnetization angles in both layers, θ_a and θ_b , may be different. Note that the coordinate system is rotated by θ_a in layer A and by θ_b in layer B . Thus the z' -axes in both layers are not parallel to each other. The respective angles are determined by the effective fields

$$\tan \theta_\alpha = \frac{B_{\alpha x}}{B_{\alpha z}} \quad (11)$$

Eq. (10) is valid as long as the deviations between the magnetization angles of different layers are small.

The coordination number within a layer is denoted by p and the structural factors $\gamma_{\mathbf{q}\parallel}$ and $\gamma_{\mathbf{q}\perp}$ are a consequence of the two dimensional Fourier transformation and depend on the lattice structure. For the fcc(100) geometry considered here they are given by

$$\begin{aligned} \gamma_{\mathbf{q}\parallel} &= 4 \cos \frac{1}{2} a q_x \cos \frac{1}{2} a q_y \\ \gamma_{\mathbf{q}\perp} &= e^{-i\frac{1}{2} a q_x} \left(2 \cos \frac{1}{2} a q_y + e^{-i\frac{1}{2} a q_x} \right), \end{aligned}$$

where a is the lattice constant.

From the single-magnon Green function (10) one can easily obtain the expectation values $\langle S_{z'} \rangle$ and $\langle S_{z'}^2 \rangle$ using the standard text book procedure²³ which can be generalized to film geometries straightforwardly.²⁴ Additionally the spin wave frequencies $h\nu_{\mathbf{q}} = E_{\mathbf{q}}$ are directly given by the eigenvalues $E_{\mathbf{q}}$ of the matrix $\mathbf{M}_{\mathbf{q}}$. Eqs. (7) - (11) establish a self consistent set of equations and thus the

problem is solved as far as the Hamiltonian (5) is concerned.

Now the dipolar term

$$H_2 = \sum_{ij\alpha} g_{0\alpha} \left(\frac{1}{r_{ij}^3} \mathbf{S}_{i\alpha} \mathbf{S}_{j\alpha} - \frac{3}{r_{ij}^5} (\mathbf{S}_{i\alpha} \mathbf{r}_{ij}) (\mathbf{S}_{j\alpha} \mathbf{r}_{ij}) \right) \quad (12)$$

has to be treated. The interaction is nonlocal and very similar to the Heisenberg exchange terms. Thus an RPA decoupling would be certainly a good choice. However it was shown in Ref. 25 that the more feasible mean field decoupling also yields acceptable results. A further term has to be added to the effective field (7) due to the dipolar coupling:

$$\mathbf{B}_\alpha = \mathbf{B}_{1\alpha} + \mathbf{B}_{\text{dip}\alpha}, \quad (13)$$

where the dipolar field is given by²⁵

$$\begin{aligned} B_{\text{dip}\alpha x} &= g_{0\alpha} \langle S_{x\alpha} \rangle \sum_j \frac{1}{r_{0j}^3} \\ B_{\text{dip}\alpha z} &= -2g_{0\alpha} \langle S_{z\alpha} \rangle \sum_j \frac{1}{r_{0j}^3}. \end{aligned} \quad (14)$$

The sum runs over all lattice sites of a layer. There are no further changes in the relations (7)- (11) due to the dipolar coupling. Thus the effective field \mathbf{B}_α defined in Eqs. (13) and (14) simply has to replace the field $\mathbf{B}_{1\alpha}$ from Eq. (7) if one wants to account for dipolar coupling.

As already mentioned before, this theory is capable of calculating the whole spin wave excitation spectrum and especially the uniform modes ω_{0o} and ω_{0a} . Therewith the resonance fields $B_{0r(a,o)}$ can be obtained for any microwave probe frequency ν_{hf} . This holds for arbitrary external field directions and for any temperature. Thus one can calculate the central functions $B_{0r(a,o)}(\theta_{B_0})$ and $B_{0r(a,o)}(T)$ as well as the dependence of the resonance frequency on the external field $\omega_{0(a,o)}(B)$. The latter is often referred to as "dispersion relation" in connection with FMR experiments and gives the excitation gap $E_{\text{gap}} = \hbar \cdot \min(\omega_{(0a)}, \omega_{(0o)})$. The results will be presented and discussed in the next section.

III. THE SINGLE FILM

In the following sections the anisotropy parameters and the dipolar coupling will be given in units of $[\mu_B \text{kG}]$ with $1 \mu_B \text{kG} = 5.79 \mu \text{eV}$. As can be seen in the Hamiltonian (2) the parameters J_I, J_α, K_2 and g_0 denote energies per lattice site, i.e. energy densities rather than energies. The external fields are given in [kG] while the resonance frequencies $\nu_0 = \omega_0/2\pi$ are given in [GHz]. The spin quantum number is set to unity ($S=1$) and the Lande factor is fixed to the bulk nickel value $g_{J_\alpha} = 2.21$. Though we are mainly interested in the coupled bilayer

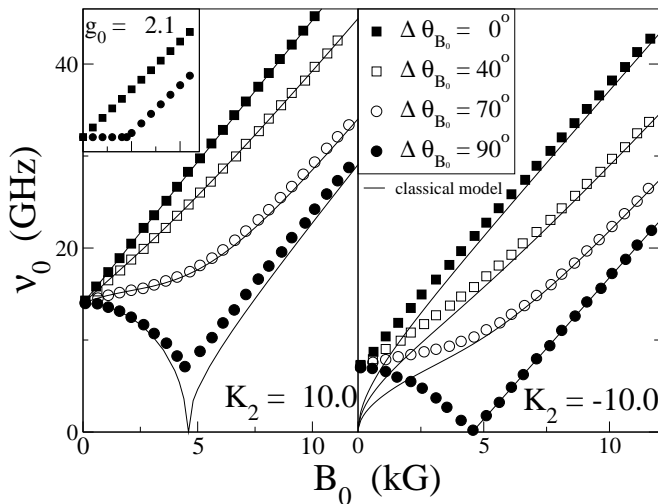


FIG. 1: The resonance frequency as a function of the external field at $T = 0$ for different angles between the easy direction and the external field $\Delta\theta_{B_0}$ (symbols). Left panel: positive lattice anisotropy $K_2 = 10 \mu_B\text{kG}$, right panel: negative lattice anisotropy $K_2 = -10 \mu_B\text{kG}$, inset: dipolar coupling $g_0 = 2.1 \mu_B\text{kG}$. Here and in the following pictures the spin quantum number is set to unity ($S=1$). The results of the classical model are also shown (solid lines).

system one has to understand the single film system before a meaningful interpretation of more complex systems is possible. Moreover, though the experimental output is the resonance field it is very instructive to study the “dispersion relation”. The dispersion relations for zero temperature are shown in Fig. 1. The spin wave frequency ν_0 is displayed as a function of the external field B_0 for positive and negative lattice anisotropies $K_2 = \pm 10 \mu_B\text{kG}$ (left and right panel, $g_0 = 0$) as well as for dipolar coupling $g_0 = 2.1 \mu_B\text{kG}$ (inset, $K_2 = 0$). The angle $\Delta\theta_{B_0}$ denotes the angle between the external field and the easy direction. The latter is perpendicular to the film for a positive lattice anisotropy and parallel to the film plane for negative lattice anisotropies or for dipolar coupling. For comparison the results of the classical model as e.g. given in Ref. 8 are also shown (thin solid lines). The anisotropy parameter \tilde{K}_2 used for the classical calculation is scaled as proposed in Ref. 26 ($\tilde{K}_2 = S(S-1/2)K_2$) and accounts for both, lattice and dipolar anisotropies. Qualitatively the results are similar for all cases. If the external field is applied parallel to the easy direction ($\Delta\theta_{B_0} = 0^\circ$) the function $\nu_0(B_0)$ increases linearly. The intersection with the ordinate gives the minimal excitation gap due to the anisotropy. This gap is larger for positive than for negative lattice anisotropies and rises with the norm of K_2 as can be seen by a comparison of the left panel of Fig. 1 ($K_2 = 10 \mu_B\text{kG}$) and the solid line in Fig. 2 ($K_2 = 15 \mu_B\text{kG}$). There are more features in the dispersion relation if the external field is applied in the hard direction ($\Delta\theta_{B_0} = 90^\circ$). The magnetization is now rotated out of its easy direction and finally aligned

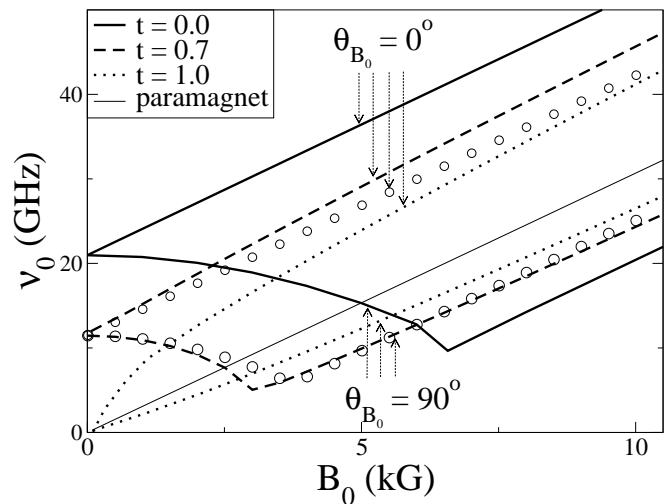


FIG. 2: The dispersion relations $\nu_0(B_0)$ at four different reduced temperatures $t = T/T_c$. The external field is applied in the easy (upper curves) and in the hard direction (lower curves). The lattice anisotropy is $K_2 = 15 \mu_B\text{kG}$ and the dipolar coupling is zero. The thin solid line gives the resonance frequencies for paramagnetism. Circles: $t = 0$, $K_2 = 8.2 \mu_B\text{kG}$

parallel to the external field if the latter exceeds a certain value called reorientation field.^{14,18} If the external field is enhanced further the magnetization does not change its orientation any more and the spin wave frequency ν_0 is again a linearly increasing function of the external field. However, before the reorientation field is reached, $\nu_0(B_0)$ is constant (for dipolar coupling) or decreases (for lattice anisotropies) as a function of the external field. There is an interesting feature for negative K_2 : at the reorientation field the resonance frequency is zero, i.e. the excitation gap is closed in spite of the presence of an external field and lattice anisotropies. This is not found for positive values of K_2 or for dipolar coupling, where the gap stays finite at the reorientation field (left panel). In such cases the probe frequency ν_{hf} may be lower than the resonance frequency ν_0 for all angles $\Delta\theta_{B_0}$ and no resonance field is detected at all. This feature is not reproduced by the classical model, but experimental evidence for such a scenario was indeed reported for nickel films with enhanced uniaxial anisotropy.¹⁷ There are more differences between the classical and quantum mechanical theory for negative anisotropies and dipolar coupling, namely for field values that are smaller than the reorientation field. Consider, for example, an external field applied perpendicularly to the easy direction ($\theta_{B_0} = 90^\circ$, dots). Here the resonance frequency and therewith the excitation gap is zero for all field values below the reorientation field in the classical calculation. The same is expected for the quantum mechanical calculation, since in this region the magnetization has a finite component parallel to the film plane in the ground state and thus the ground state is degenerated with respect to

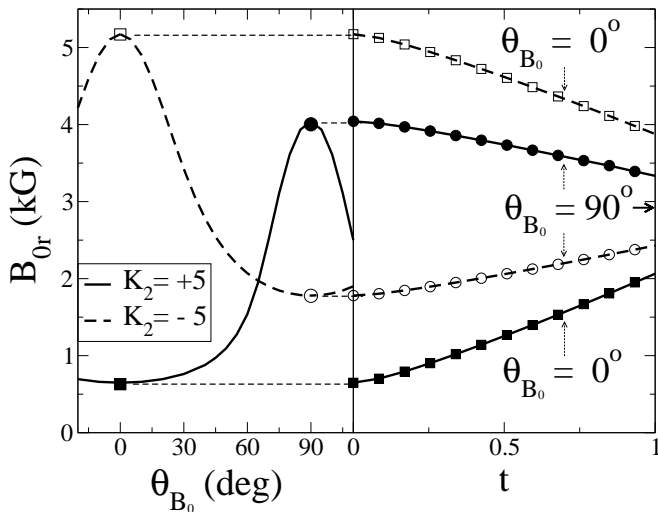


FIG. 3: The resonance fields for positive (solid lines, filled symbols) as well as for negative (dashed lines, open symbols) lattice anisotropies as a function of the polar angle of the external field (left panel, $T = 0$) and as a function of reduced temperature $t = T/T_c$ (right panel, $\theta_{B_0} = 0^\circ$ - squares, $\theta_{B_0} = 90^\circ$ - circles). The position of the resonance field of a paramagnet is indicated by the arrow in the right panel.

the azimuthal angle ϕ of the magnetization. Therefore a Goldstone mode is expected, i.e. the spin-wave energy for $q = 0$ should be zero. This feature is not reproduced by our approximation, since it restricts the problem to a plane perpendicular to the film plane. However, despite these differences, the agreement between the classical and the microscopic theory is rather good for a large region of the parameter space at $T = 0$.

Let us now consider the temperature dependence of the dispersion relation. In the following discussion the external field will be applied either along the easy direction or along the hard direction. This configurations will be referred to shortly as “easy direction” or “hard direction” case. In Fig. 2 we display the dispersion relation for positive K_2 at three different reduced temperatures $t = T/T_c$ ranging from $t = 0.0$ to $t = 1.0$ for the easy as well as for the hard direction case. Additionally the result for a reduced anisotropy $K'_2 = 0.547K_2$ at zero temperature $t = 0$ is shown (circles). The thin solid line denotes the resonance as found for a paramagnet ($J_\alpha = 0$). The dispersion relation shows a significant temperature dependence: With increasing t the curves move towards the paramagnetic line. The *magnitude* of this shift in a certain temperature interval is determined by the distance between the spin wave frequency at $t = 0$ and the paramagnetic mode. The resonance frequencies for the easy direction case are more sensitive to temperature than those for the hard direction case, since the former are further away from the paramagnetic line. However, the paramagnetic solution is not reached at T_c since a finite magnetization is induced by the external field. Further one notices that the shape of the curves at $t = 0$ and at $t = 0.7$

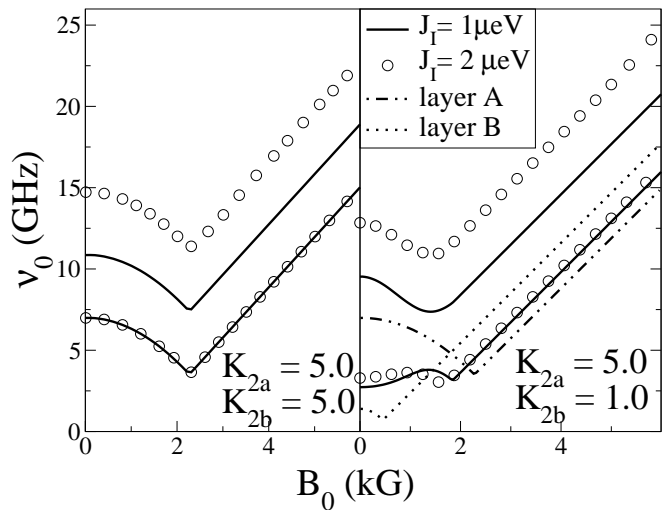


FIG. 4: The resonance frequencies as a function of the external field applied in the hard direction for a coupled bilayer system. Left: symmetric film system, $K_{2a} = K_{2b} = 5 \mu_B kG$, right: Asymmetric film system $K_{2a} = 5K_{2b} = 5 \mu_B kG$. For both panels the interlayer coupling strengths are $J_I = 1 \mu eV$ (solid lines) and $J_I = 2 \mu eV$ (circles). Additionally the results for single films, i.e. $J_I = 0$ are shown in the right panel (dash-dotted line - layer A and dotted line - layer B).

are qualitatively the same. Temperature reduces the resonance frequency for zero external field as well as the re-orientation field. Similar effects are found for fixed temperature but reduced anisotropy constant K_2 as can be seen by comparing the results for $K_2 = 15 \mu_B kG$, $t = 0.7$ (dashed line) and $K_2 = 8.2 \mu_B kG$, $t = 0$ (circles). However, there are still differences between both cases and hence a reduced anisotropy parameter has clearly not the same effects on the dispersion relation as increasing temperature. The curves for temperatures in the vicinity or above the Curie temperature and for $t = 0$ differ even qualitatively. Similar results are found for negative lattice anisotropies and for dipolar coupling. These findings bear important consequences for the usual interpretation of FMR data in terms of a classical model where the effect of temperature is taken into account via effective anisotropy parameters $\tilde{K}_2(T)$. Obviously, this ansatz is an acceptable approximation only for lower temperatures and not at all justified for temperatures in the vicinity or above T_c .

At the end of this section we want to discuss resonance fields (Fig. 3). The angular as well as the temperature dependence is shown for positive (solid line, filled symbols) as well as for negative (dashed line, open symbols) lattice anisotropies. A probe frequency of 9 GHz is chosen. It is clearly seen that the resonance field has a maximum at the hard direction and a minimum at the easy direction. The resonance fields at these extremal points are larger for negative than for positive anisotropies.

If the temperature is enhanced, the resonance fields shift towards the paramagnetic limit $B_{0r}(\text{param}) = 2.9 \text{ kG}$,

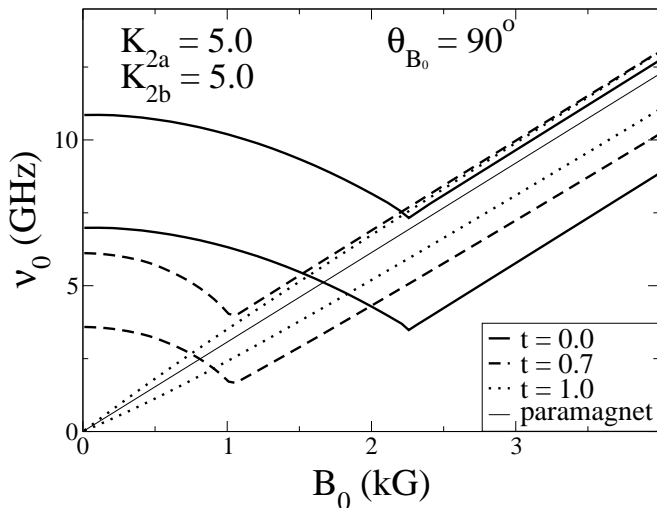


FIG. 5: The dispersion relations for a symmetric film system ($K_{2(a,b)} = 5 \mu_B \text{kG}$, $J_I = 1 \mu\text{eV}$) for different reduced temperatures $t = T/T_c$. The external field is applied in the hard direction. The paramagnetic solution is also shown (thin solid line).

which is however not reached before $t \approx 2.5$. Again the magnitude of these shifts in a certain temperature interval scale with the distance between the resonance field at zero temperature and the resonance field found for a paramagnet. Thus for both signs of the anisotropy the temperature dependence of the resonance field is more pronounced if the external field is applied perpendicularly to the film plane rather than parallelly. The resonance fields increase with temperature in the easy direction and decrease with temperature in the hard direction. All characteristic features follow from the respective dispersion relations in Fig. 1 and Fig. 2. Keeping in mind the behavior of the single film we now want to analyze the coupled bilayer system to understand the intrinsic temperature dependence of the interlayer exchange coupling. Concerning the coupled system we will consider two cases: a symmetric film system where the upper and the lower layers are equivalent and an asymmetric film system, i.e. a system with different anisotropy strengths in the upper and the lower layer.

IV. THE INTERLAYER COUPLING

We start our discussion considering dispersion relations. Fig. 4 shows the dispersion relation of two equivalent layers (left panel, $K_{2a} = K_{2b} = 5 \mu_B \text{kG}$) as well as of an asymmetric film system (right panel, $K_{2a} = 5 \mu_B \text{kG}$, $K_{2b} = 1 \mu_B \text{kG}$). The interlayer couplings are $1 \mu\text{eV}$ (solid lines) and $2 \mu\text{eV}$ (circles), the temperature is zero. For the asymmetric system the results for decoupled films ($J_I = 0$) is also shown. The easy direction is perpendicular to the film and the external field is applied in the hard direction. For the coupled

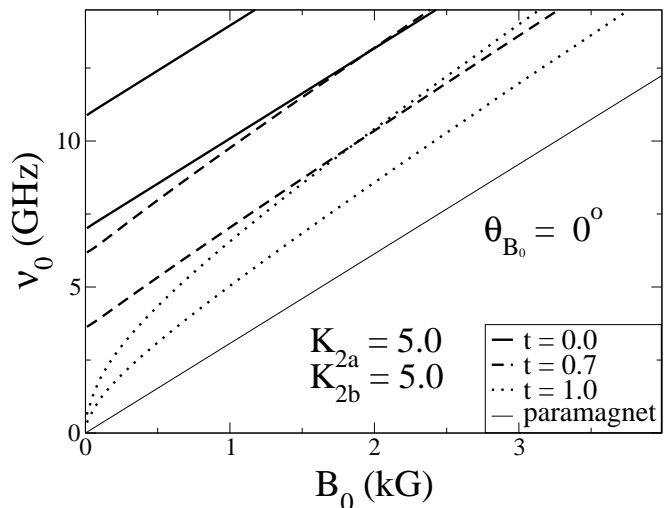


FIG. 6: The same as Fig. 5, but for an external field applied in the easy direction ($\theta_{B_0} = 0^\circ$).

film two modes are found, the acoustical (lower) and the optical one (upper). In the case of symmetric parameters the curves are parallel and the distance between the modes $\Delta\nu_0$ scales with the interlayer coupling strength J_I . The position of the acoustical mode is not influenced by the interlayer coupling strength. The same applies for the easy direction case. The situation is somewhat more complex if the layers are not equivalent as shown in the right panel. For $B_0 = 0$ the modes have lower frequencies compared to the symmetric system. This is caused by the reduced anisotropy strength in layer b . Furthermore the modes are not parallel any more and the distance between the modes depends on both: the film asymmetry and the interlayer coupling. Other than for symmetric films the acoustical mode is now slightly influenced by the interlayer coupling strength J_I . It is located between the modes of the upper and the lower layer of the decoupled system.

Next we want to analyze the temperature dependence of the resonance modes at fixed anisotropy and interlayer coupling parameters. Note that this is not possible within the classical theory,^{10,11} where different anisotropy parameters and interlayer coupling constants have to be assumed for every temperature. Fig. 5 and Fig. 6 show the dispersion relations for equivalent layers at three different reduced temperatures: $t = 0.0$, $t = 0.7$ and $t = 1.0$ for the easy and the hard direction case as well as the dispersion relation of a paramagnet (thin solid lines). Similar trends as for the single layer are found for the temperature dependence of the resonance frequencies. All modes move towards the paramagnetic solution with increasing temperature and the magnitudes of the shifts scale with the distance to the paramagnetic mode. For the hard direction case (Fig. 5) the optical mode is influenced only slightly in the linear regime, since the distance to the paramagnetic mode is very small. Because in this regime this distance is larger for the acoustical

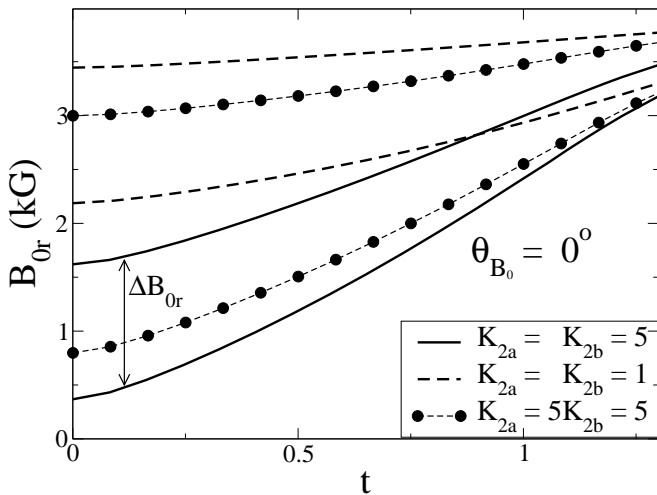


FIG. 7: The resonance fields as a function of temperature for the easy direction. The results of two symmetric film systems ($K_{2a} = K_{2b} = 5 \mu_B \text{kG}$ - solid lines, $K_{2a} = K_{2b} = 1 \mu_B \text{kG}$ - dashed lines) as well as of an asymmetric film system ($K_{2a} = 5K_{2b} = 5 \mu_B \text{kG}$ - dashed lines with circles) are shown. Further parameters: $J_I = 1 \mu\text{eV}$, $\nu_0 = 12 \text{GHz}$.

mode the latter is stronger influenced by temperature. For zero external field the mode frequencies of the optical and acoustical mode get smaller with increasing temperature and reach zero at T_c . The distance between the optical and acoustical mode is clearly reduced by increasing temperature but stays finite for finite fields at the Curie temperature. For the easy direction case (Fig. 6) the $t = 0$ resonance frequencies of both modes are clearly larger than the paramagnetic one. This causes a significant decrease of the resonance frequencies with increasing temperature. The distance between the modes $\Delta\nu_0$ is reduced with temperature. This reduction is comparable in the easy and in the hard direction case.

Let us now consider the temperature dependence of the resonance fields for the coupled bilayer system. The probe frequency is chosen to be 12 GHz. The resonance field for a paramagnet is $B_{0r}(\text{param}) = 3.87 \text{kG}$. Fig. 7 (easy direction) and Fig. 8 (hard direction) show the resonance fields as a function of temperature for ferromagnetic interlayer coupling ($J_I = 1 \mu\text{eV}$). Two symmetric films with higher ($K_2 = 5 \mu_B \text{kG}$ - solid lines) and smaller anisotropy strength ($K_2 = 1 \mu_B \text{kG}$ - dashed lines) as well as an asymmetric film system (symbols) are considered. In the easy direction case all resonance fields are smaller than the paramagnetic solution and therefore the fields increase with temperature. For zero temperature the resonance fields are smaller for larger anisotropy strengths. The mode distance, however, is the same for both symmetric systems ($\Delta B_{0r} \approx 1.25 \text{kG}$). It is clearly seen that the asymmetric system is somehow a "mixture" between the considered symmetric systems. The acoustical as well as the optical resonance fields are located between the respective fields of the symmetric systems. The resulting distance between the optical and the acoustical field is

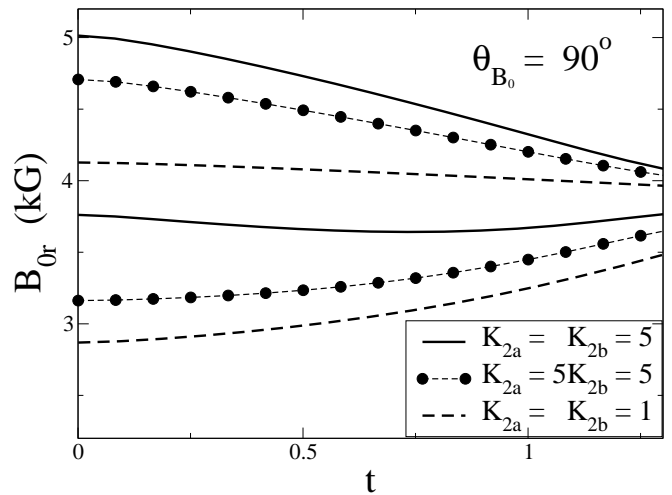


FIG. 8: The same as Fig. 7, but for external fields applied in the hard direction.

larger than for the symmetric systems. This is in agreement to the findings of Fig. 4. Since the resonance fields for higher anisotropies are further away from the paramagnetic solution they react more sensitively to temperature than the resonance fields for the low anisotropy system. The distance between the modes is reduced by temperature for all considered systems.

The behavior in the hard direction case is similar. The acoustical resonance fields are larger than the paramagnetic one and consequently the fields are reduced by temperature. The resonance fields of the optical mode increase with temperature for the low anisotropy and for the asymmetric film system since they are smaller than the paramagnetic field. If the resonance field is very close to the paramagnetic one the resonance field may behave non monotonically as found for the optical resonance of the high anisotropy system (lower solid line). As for the easy direction case the distance between the optical and acoustical resonance field ΔB_{0r} is reduced by temperature. The last point is of special interest for symmetric systems. Recall that for zero temperature as well as within the classical approach^{10,11} the distance between the optical and acoustical field ΔB_{0r} is solely determined by the interlayer coupling strength. This feature, however, is lost at finite temperatures. As can be seen in Fig. 9 the distance shrinks faster for the high anisotropy system $K_2 = 5 \mu_B \text{kG}$ than for the system with lower anisotropy $K_2 = 1 \mu_B \text{kG}$, irrespective of the same interlayer coupling strength. Thus the field distance ΔB_{0r} depends on both, on the interlayer coupling strength as well as on the anisotropies. Note that for finite temperatures this holds even for symmetric systems, i.e. systems with equivalent magnetic films. This behavior is not reproduced by the classical theory^{10,11}. For the asymmetric system the temperature dependence is comparable to those of the high anisotropy system. Furthermore the temperature dependence of the distance between the optical and acoustical field ΔB_{0r} is slightly enhanced for

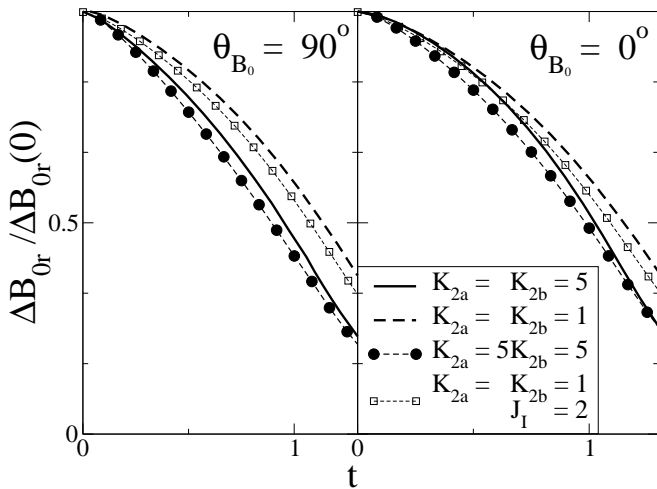


FIG. 9: The distance between the optical and acoustical resonance field ΔB_{or} as a function of the reduced temperature $t = T/T_c$ normalized to its $t = 0$ value. For $J_I = 1 \mu\text{eV}$ results are shown for a symmetric system with a lower anisotropy (dashed line), for a symmetric system with a higher anisotropy (solid line) and an asymmetric film system with a high anisotropy layer and a low anisotropy layer (filled dots). For $J_I = 2 \mu\text{eV}$ results are shown for the symmetric low anisotropy system (open squares).

higher coupling strengths (open squares).

Let us summarize our findings for the coupled bilayer system:

- There are two uniform modes belonging to the acoustical and optical spin wave branch for the coupled bilayer system. For equivalent layers and at $t = 0$ the mode distance $\Delta\nu_0$ is a measure for the interlayer coupling strength.
- Both modes and the respective resonance fields are shifted towards the paramagnetic solution with increasing temperature. The magnitude of these shifts is determined by the distance of the respective mode from the paramagnetic line. The distance between the optical and acoustical mode $\Delta\nu_0$ and the distance between the resonance fields ΔB_{or} are reduced by temperature.
- The magnitudes of these reductions are found to be larger for systems with a larger anisotropy strength.

The temperature dependence of the resonance frequencies and fields is reflected in the temperature dependence of the effective interlayer coupling $\tilde{J}_I(T)$ if the latter is obtained from experiment. It is clear that the effective interlayer coupling $\tilde{J}_I(T)$ decreases if the temperature is enhanced. The magnitude of this decrease, however, may depend on the anisotropies of the film and is larger for larger anisotropies. Note that this behavior is exclusively due to the contribution of spin wave interactions to the temperature dependence of the uniform mode.

V. CONCLUSIONS AND OUTLOOK

Commonly there are two methods used to evaluate FMR experiments, namely a method based on an expansion of the free energy¹¹ or a method based on the equation of motion for the classical magnetization vector.¹⁰ Both techniques use a classical continuum model. In this paper we propose an alternative method based on an extended microscopic Heisenberg model. The theoretical treatment of this model was shown to give excellent results for arbitrary directions of the external field.¹⁸ This new approach allows for an explicit consideration of temperature as far as magnetic excitations are concerned. We used the theory to make general predictions about the temperature dependence of the FMR frequencies and fields caused by magnetic excitations. Additionally the results of the new method were compared to results of the classical model. A single film as well as an interlayer coupled bilayer system were considered. We found the following results:

- For zero temperature the results of the new method are very similar to those of the classical model for many parameter settings. There is however an important difference in the hard direction: The resonance frequency stays finite for all external fields for positive lattice anisotropies, while the classical model predicts a vanishing resonance frequency at the reorientation field. That is why the classical model can not explain the absence of a resonance field in the hard direction which was, however, observed experimentally for some systems.¹⁷ Using the microscopic analysis this observation turns out to be the natural consequence of the finite frequency minimum in the dispersion relation (see left panel of Fig. 1). For large anisotropy parameters the probe frequency is lower than the minimal resonance frequency and no resonance field can be detected any more.
- For the coupled bilayer system two modes are found. For $t = 0$ and equivalent magnetic layers the distance between the modes is solely determined by the interlayer coupling strength. For a system with non-equivalent layers the mode distance depends on the interlayer coupling as well as on the asymmetry of the film system.
- The resonance frequencies and fields have a significant temperature dependence. The dispersion relation looks qualitatively similar for temperatures below T_c . The frequency for zero external field as well as the minimum of the dispersion relation are shifted to lower values with increasing t . This effects are similar, but not equivalent, to a reduction of the anisotropy parameter (see Fig. 2). For temperatures in the vicinity or above T_c the shape of the dispersion relation changes drastically compared to $t = 0$.

- With increasing temperature the resonance frequencies and fields are shifted towards the paramagnetic solution. This applies for the optical as well as for the acoustical branch and causes a decrease of the distance between the optical and acoustical mode $\Delta\nu_0$ as well as of the distance between the respective resonance fields ΔB_{0r} . However, the paramagnetic solution is not reached at T_c since the external field induces a finite magnetization above T_c .
- For symmetric films the behavior of ΔB_{0r} is noteworthy. At $t = 0$ it is solely determined by the interlayer coupling strength J_I . However, the anisotropy parameters do influence the temperature dependence of ΔB_{0r} . The latter decreases faster with temperature for larger anisotropies. This qualitatively different behavior of the mode distance for zero and finite temperatures can not be described by the classical approach.

These are the trends concerning the temperature dependence of the FMR signals due to the interaction of spin waves.

Furthermore we expect valuable insights, if our model is used to analyze temperature dependent FMR measure-

ments. Concerning the temperature dependence of the interlayer exchange coupling this method can be used to separate the different mechanisms which are known to be present in such systems, namely the spacer effect due to a smearing out of the Fermi surface within the spacer and the magnetic effect caused by the excitation and interaction of spin waves. The relevance of both effects is intensively discussed in literature but a separation and thus a direct comparison of both effects was not possible up to now. Such calculations are intended for the future. Additionally the procedure can be used to analyze temperature dependent FMR measurements of anisotropy parameters.²⁷ Again the temperature dependence due to spin waves can be separated from other sources of temperature dependence which opens the possibility to gain a deeper understanding of anisotropy effects, too.

Acknowledgments

This work is supported by the Deutsche Forschungsgemeinschaft within the Sonderforschungsbereich 290. Productive discussions with K. Baberschke and his group are gratefully acknowledged.

-
- ¹ see e.g. P. Bruno, Phys. Rev. B **52**, 411 (1995).
- ² J. Mathon, M. Villeret, A. Umerski, R. B. Muniz, J. d'Albuquerque e Castro, and D. M. Edwards, Phys. Rev. B **56**, 11797 (1997).
- ³ S. Schwieger and W. Nolting, Phys. Rev. B **69**, 224413 (2004).
- ⁴ P. Bruno and C. Chappert, Phys. Rev. Lett. **67**, 1602 (1991).
- ⁵ D. M. Edwards, J. Mathon, R. B. Muniz, and M. S. Phan, Phys. Rev. Lett. **67**, 493 (1991).
- ⁶ J. d'Albuquerque e Castro, J. Mathon, M. Villeret, and A. Umerski, Phys. Rev. B **53**, R13306 (1996).
- ⁷ N. S. Almeida, D. L. Mills, and M. Teitelman, Phys. Rev. Lett. **75**, 733 (1995).
- ⁸ J. Lindner and K. Baberschke, J. Phys.:Condens. Matter **15**, R193 (2003).
- ⁹ J. Lindner and K. Baberschke, J. Phys.:Condens. Matter **15**, S465 (2003).
- ¹⁰ C. Kittel, Phys. Rev. **71**, 270 (1947); Phys. Rev. **73**, 155 (1948); Phys. Rev. **76**, 743 (1949).
- ¹¹ J. Smit and H. G. Beljers, Philips Res. Rep. **10**, 113 (1955).
- ¹² J. Lindner, C. Rüdte, E. Kosubek, P. Pouloupoulos, K. Baberschke, P. Blomquist, R. Wäppling, and D. L. Mills, Phys. Rev. Lett. **88**, 167206 (2002).
- ¹³ K. Baberschke, Appl. Phys. A **62**, 417 (1996).
- ¹⁴ see e.g. P. J. Jensen and K. H. Bennemann, in *Magnetism and electronic correlations in local-moment systems: rare earth elements and compounds*, p. 113 (World Scientific, Singapore, 1998).
- ¹⁵ of course also other quantities, as e.g. the linewidth are an interesting experimental output. However, in this paper we will exclusively consider resonance fields and frequencies.
- ¹⁶ V. Drchal, J. Kudrnovsky, P. Bruno, I. Turek, P. H. Dederichs, and P. Weinberger, Phys. Rev. B **60**, 9588 (1999).
- ¹⁷ J. Lindner, PhD Thesis FU-Berlin (2003) Dissertation.de-Verlag im Internet GmbH.
- ¹⁸ S. Schwieger, J. Kienert, and W. Nolting, Phys. Rev. B, in press, cond-mat/0411549.
- ¹⁹ P. Henelius, P. Fröbrich, P. J. Kuntz, C. Timm, and P. J. Jensen, Phys. Rev. B **66**, 094407 (2002).
- ²⁰ N. N. Bogolyubov and S. V. Tyablikov, Soviet. Phys. – Doklady **4**, 589 (1959).
- ²¹ H. Callen, Phys. Rev. **130**, 890 (1963).
- ²² F. B. Anderson and H. Callen, Phys. Rev. **136**, A1068 (1964).
- ²³ See e.g. R. A. Tahir-Kheli and D. ter Haar, Phys. Rev. **127**, 88 (1962); S. V. Tyablikov, "Quantentheoretische Methoden des Magnetismus", (Teubner, Stuttgart, 1969) or Ref. 21.
- ²⁴ R. Schiller and W. Nolting, Solid State Commun. **110**, 121 (1999).
- ²⁵ P. Fröbrich, P. J. Jensen, P. J. Kuntz, and A. Ecker, Eur. Phys. J. B, **18**, 579 (2000).
- ²⁶ P. Fröbrich, P. J. Jensen, and P. J. Kuntz, Eur. Phys. J. B, **13**, 477 (2000).
- ²⁷ M. Farle, Rep. Prog. Phys. **61**, 755 (1998).